Electronic Supplementary Material (ESI) for Inorganic Chemistry Frontiers.

Supporting Information

New "elbow-shaped" Ru(II) complexes as photoprobes and photoreactants for mismatched DNA

Quentin Deraedt, Lionel Marcélis, Frédérique Loiseau, Benjamin Elias*

Table of contents

1. Absorption spectra of the ligands

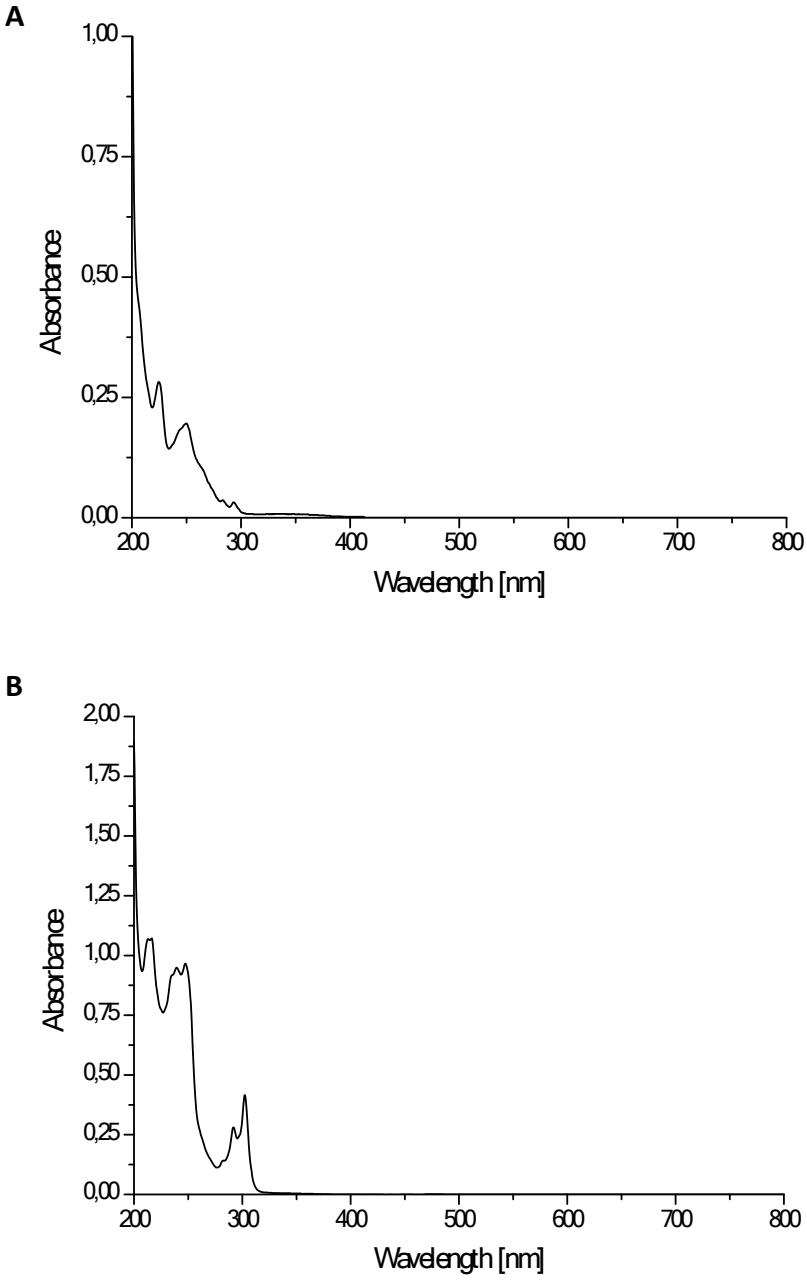

Figure S1. Absorption spectra under air in acetonitrile for (A) **1** and (B) **2**.

2. Absorption and emission spectra of the Ru(II) complexes

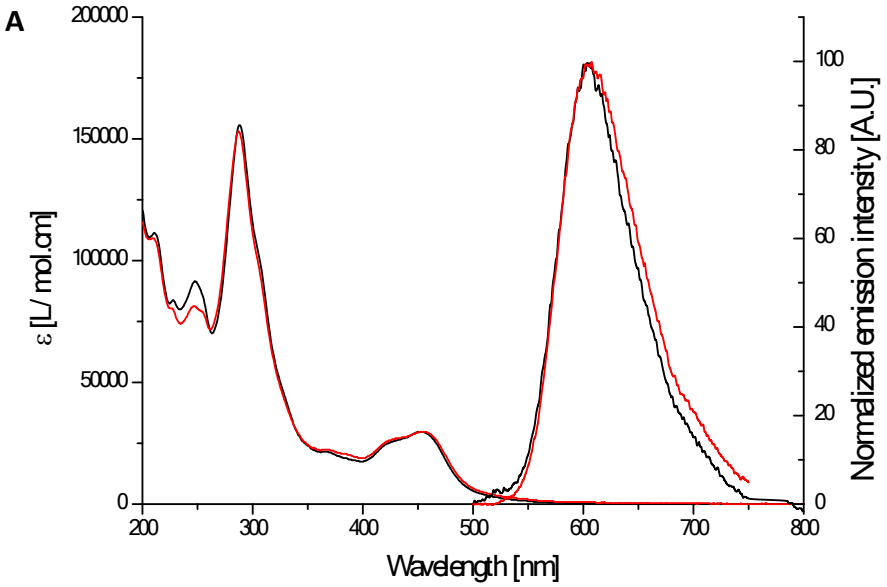

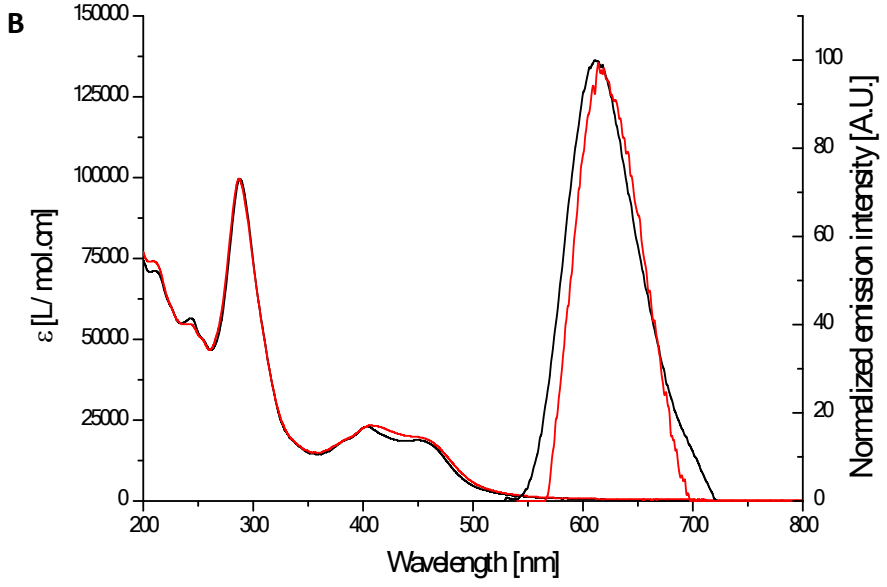

C

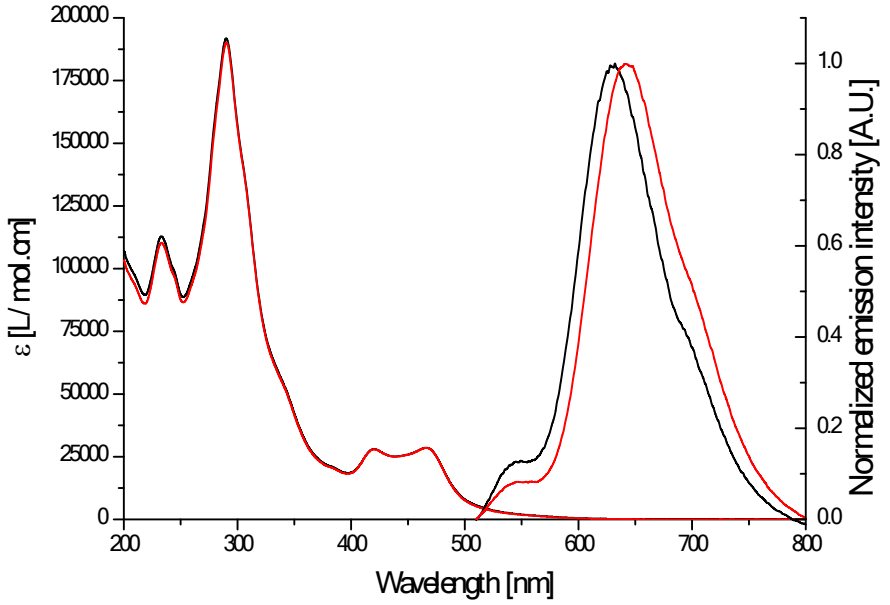
ε [L/ mol.cm]
Normalized emission intensity [A.U.]
Wavelength [nm]
200000
175000
150000
125000
100000
75000
50000
25000
0
1.0
0.8
0.6
0.4
0.2
0.0
200
300
400
500
600
700
800

D

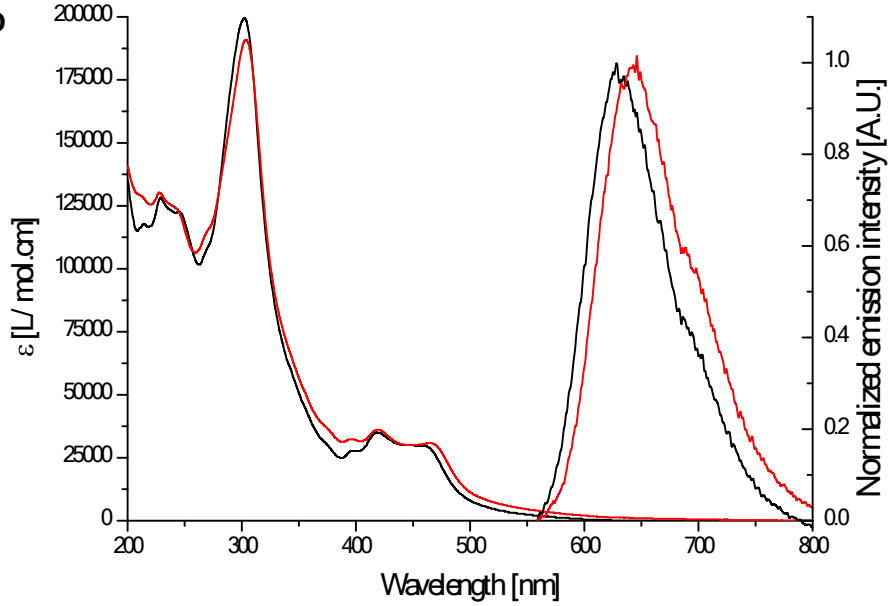
ε [L/ mol.cm]
Normalized emission intensity [A.U.]
Wavelength [nm]
200000
175000
150000
125000
100000
75000
50000
25000
0
1.0
0.8
0.6
0.4
0.2
0.0
200
300
400
500
600
700
800

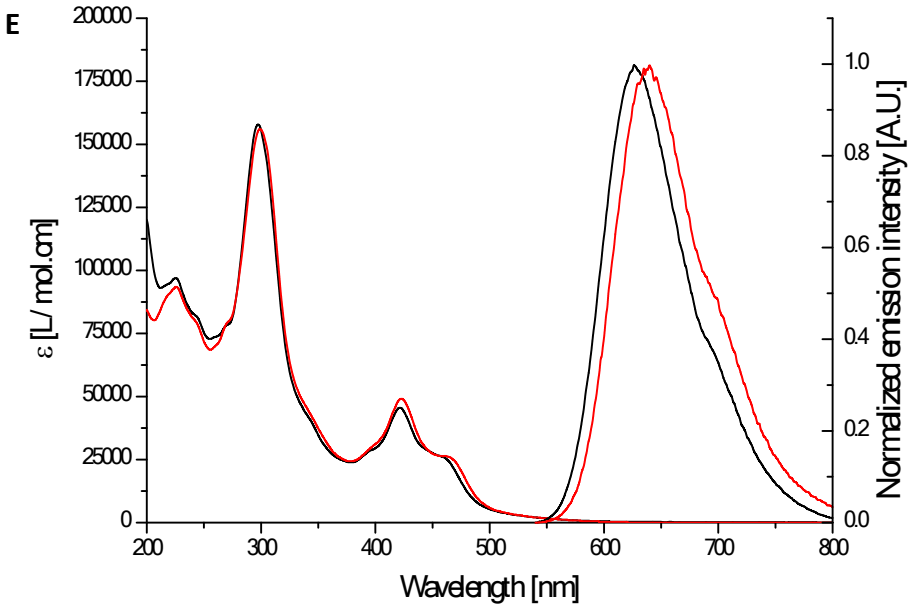

Figure S2. Absorption and emission spectra under air in acetonitrile (black) and in water (red) for (A) **1**, (B) **2**, (C) **3**, (D) **4** and (E) **5**.

3. Emission spectra of the Ru(II) complexes at 77K

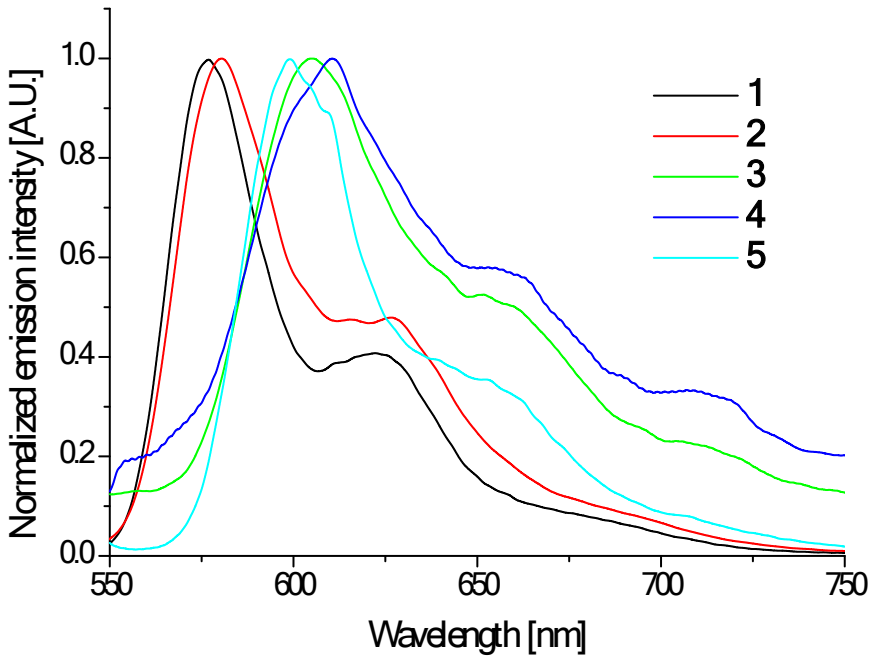

Figure S3. Emission spectra at 77K in EtOH/MeOH 4/1 (v/v) rigid matrix for **1** (black), **2** (red), **3** (green), **4** (blue) and **5** (cyan).

4. Synthetic schemes

4.1. Synthesis of bpy-based Ru(II) complexes and their related ligands

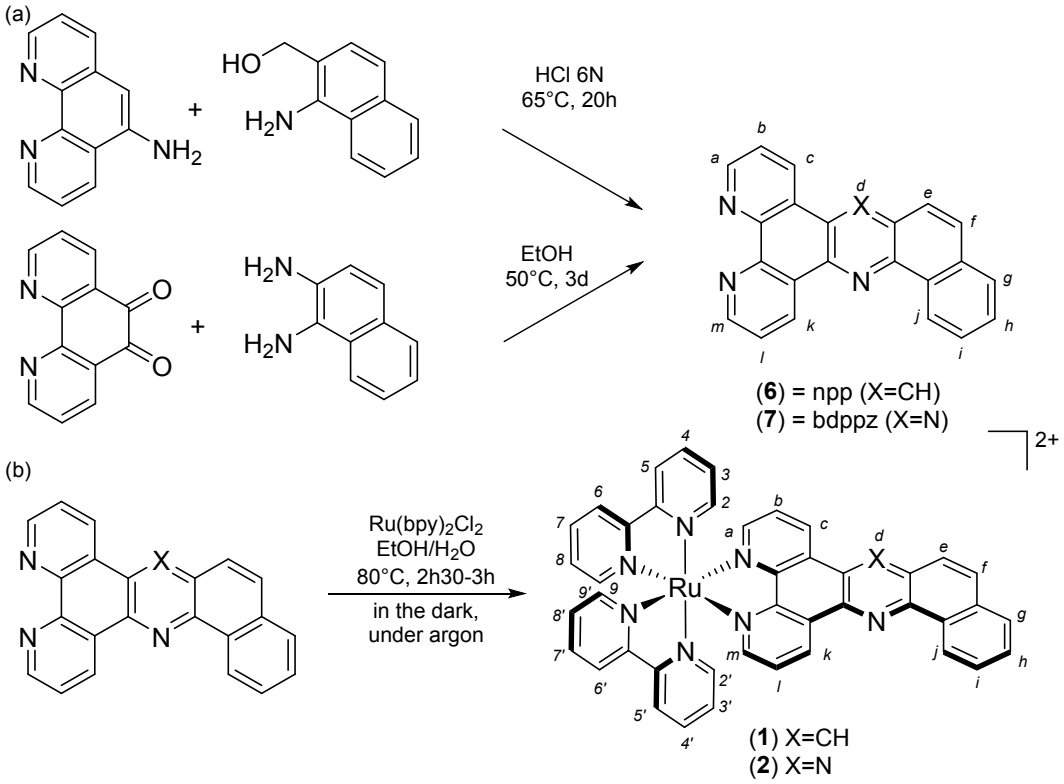

Figure S4. Synthetic scheme for complexes **1**-**2** and ligands **6**-**7**.

4.2. Synthesis of bpz-based Ru(II) complexes

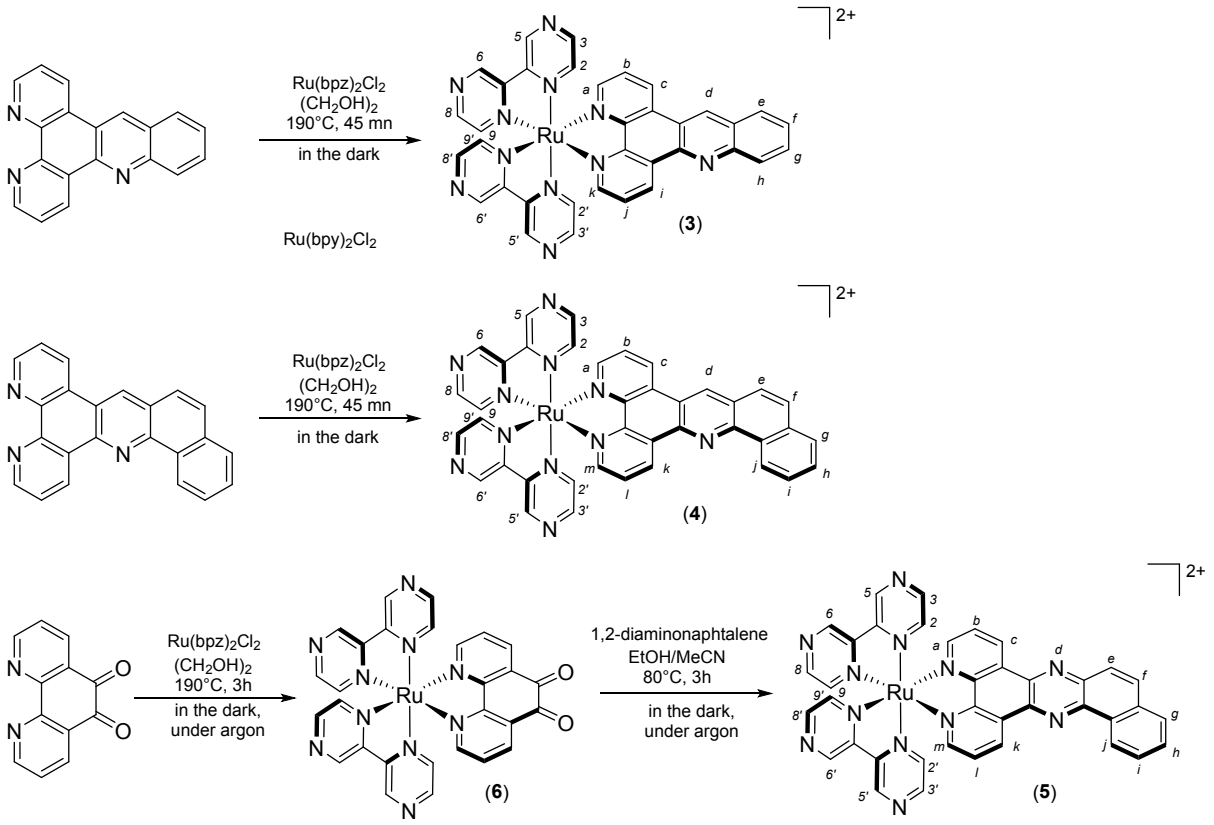

Figure S5. Synthetic scheme for complexes **3**-**5**.

5. ^{1}H-NMR spectra

5.1. ^{1}H-NMR spectra of the ligands

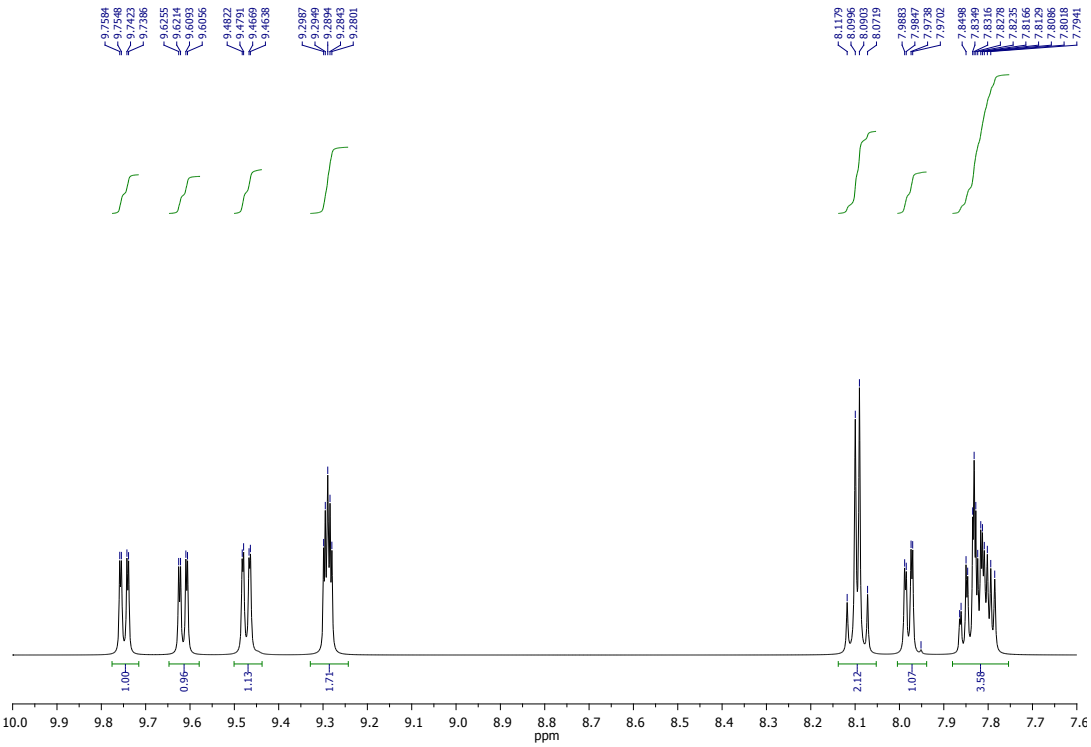

Figure S6. ^{1}H-NMR spectrum for **7** (500 MHz, $CDCl_3$).

5.2. ^{1}H and 2D NMR spectra of the Ru(II) complexes

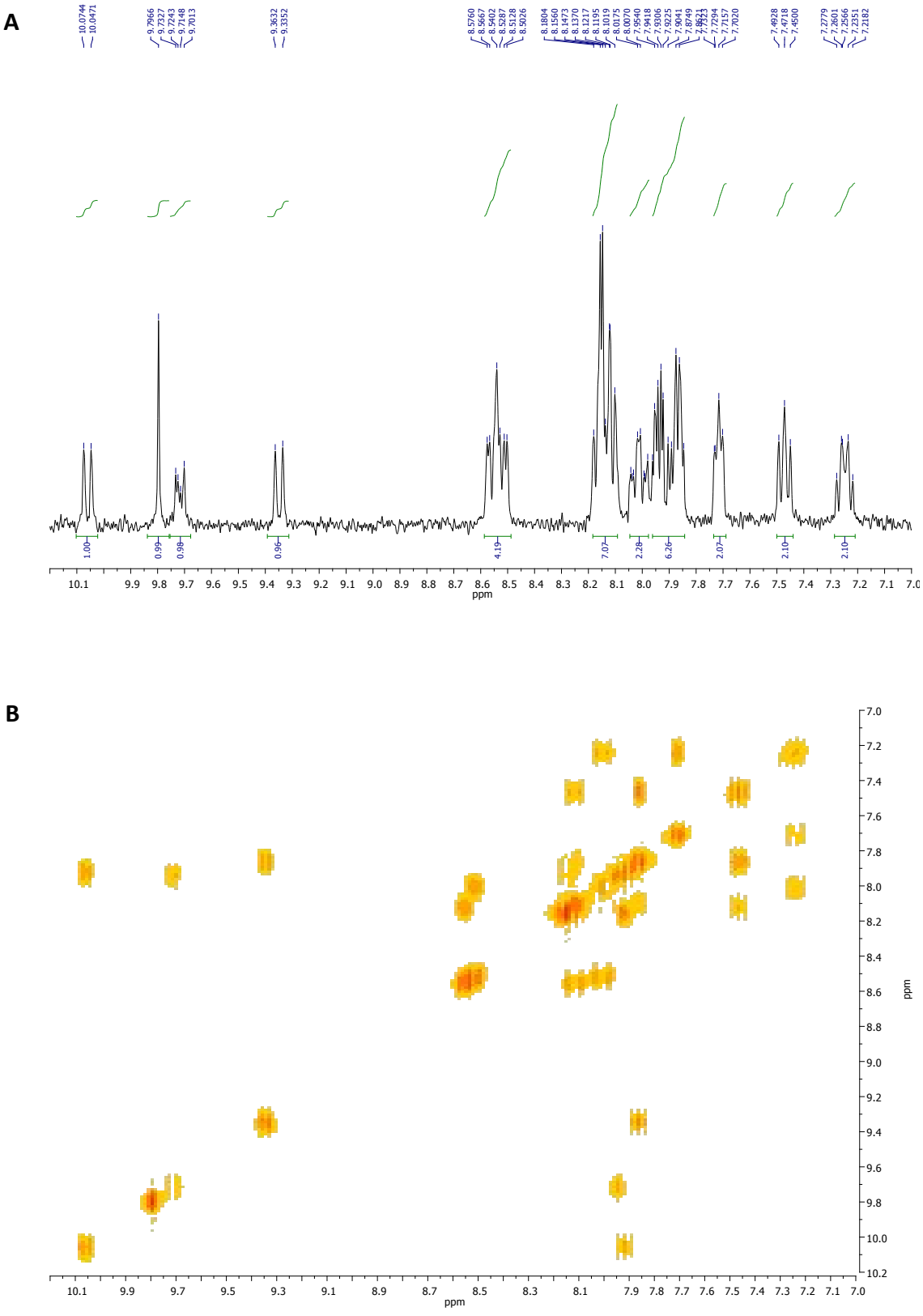

Figure S7. (A) 1D and (B) 2D ^{1}H-NMR spectra for **1** (300 MHz, CD_3CN).

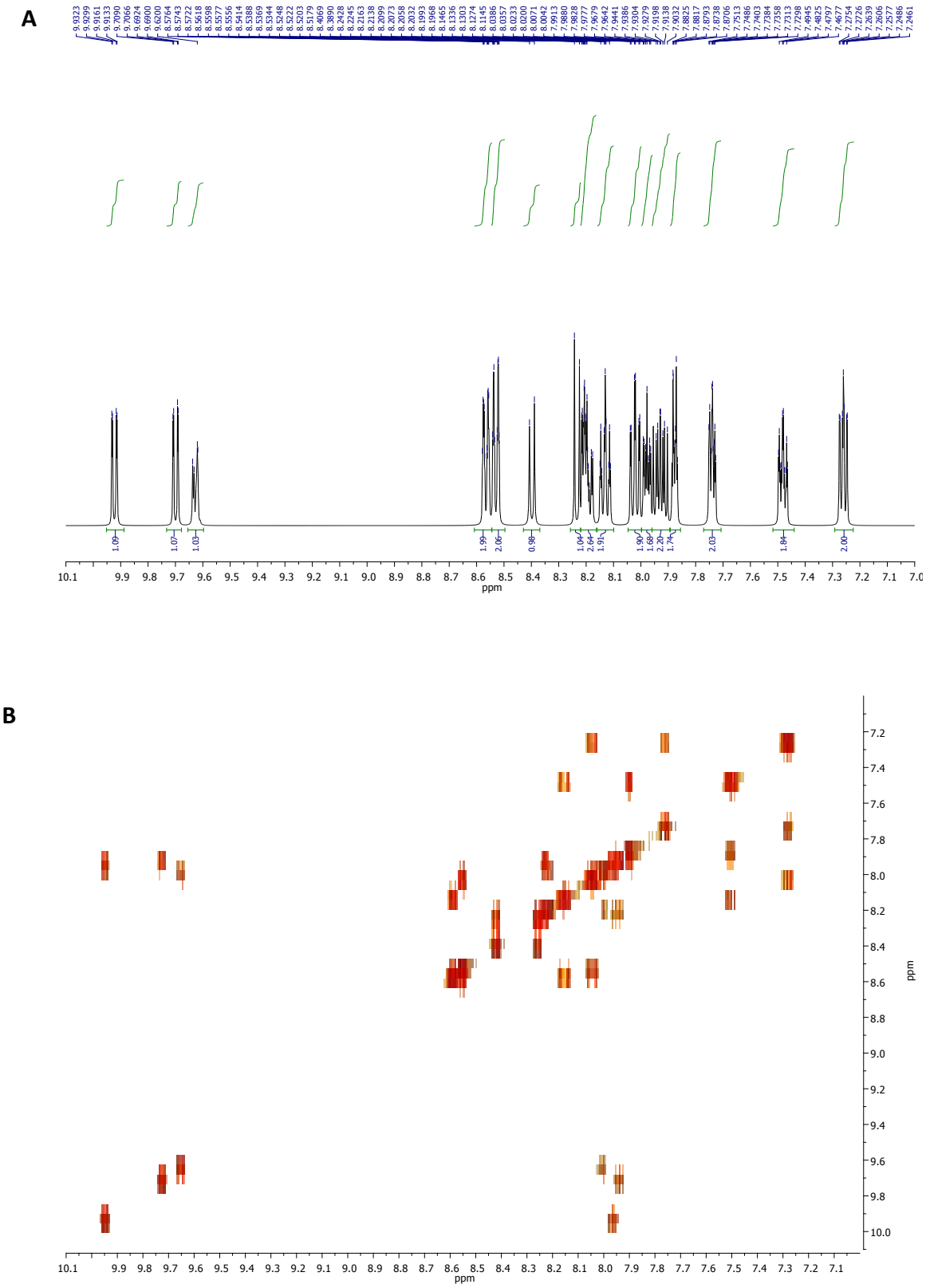

Figure S8. (A) 1D and (B) 2D ^{1}H-NMR spectra for **2** (500 MHz, CD_3CN).

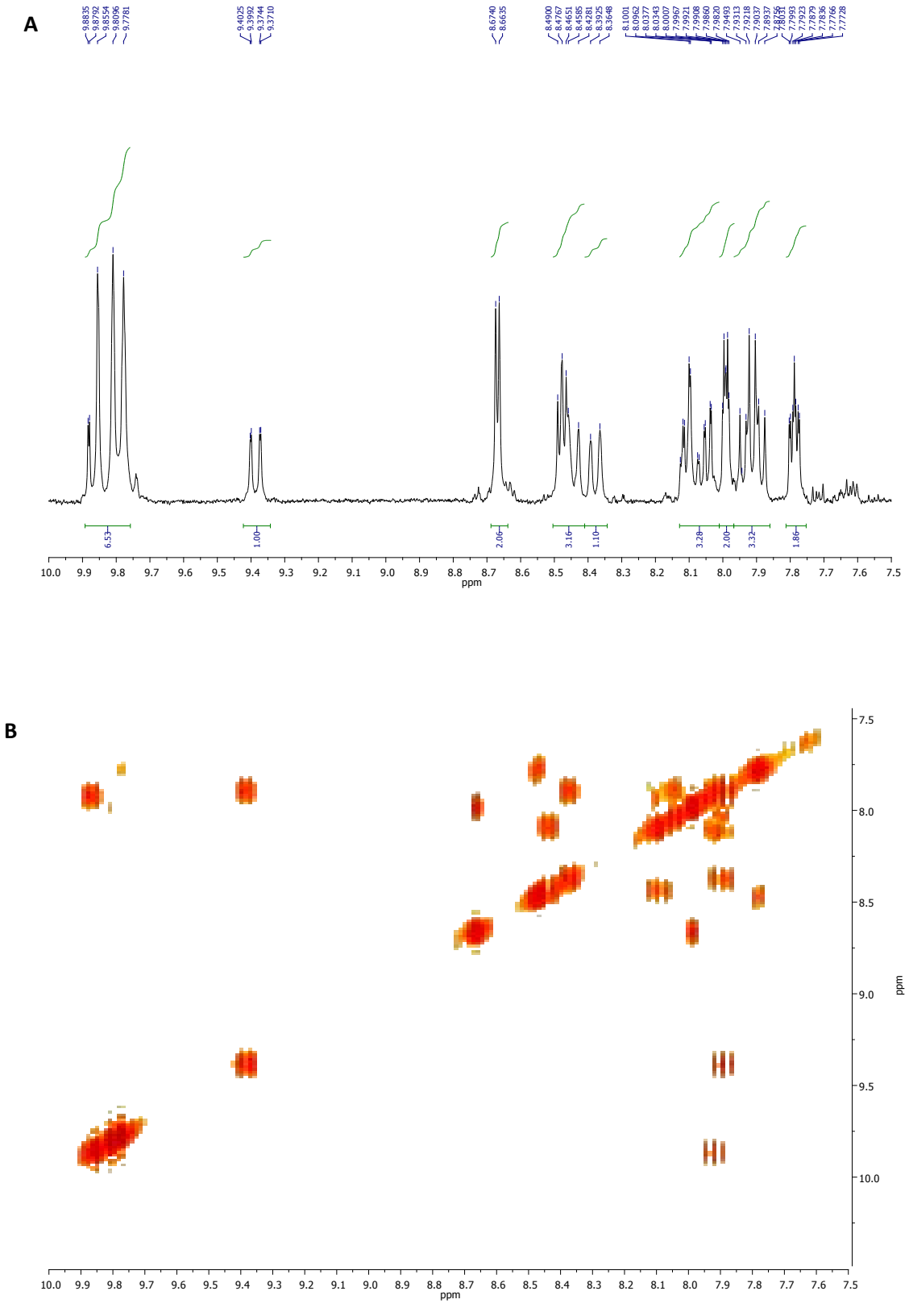

Figure S9. (A) 1D and (B) 2D ^{1}H-NMR spectra for **3** (300 MHz, CD_3CN).

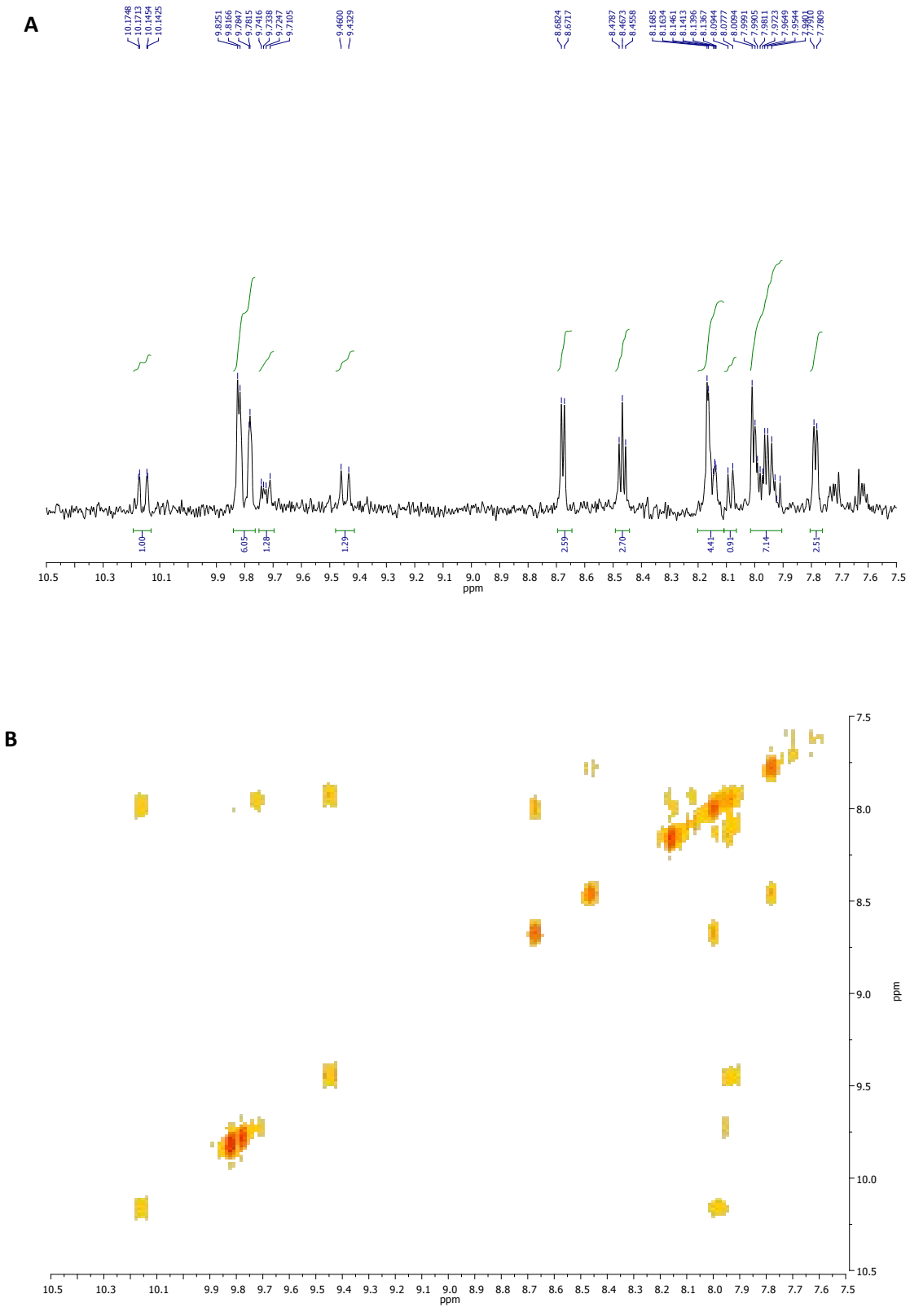

Figure S10. (A) 1D and (B) 2D ^{1}H-NMR spectra for **4** (300 MHz, CD_3CN).

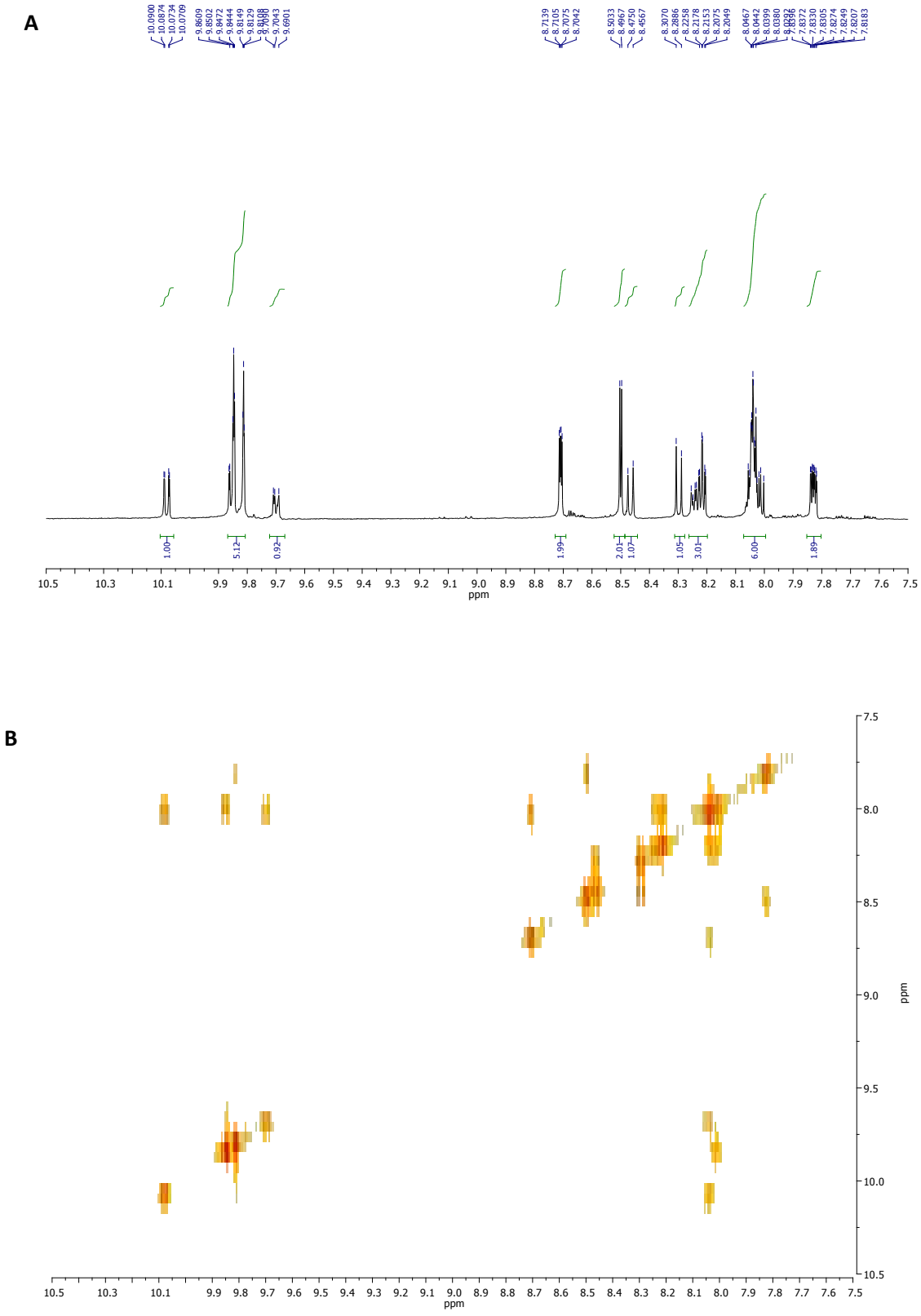

Figure S11. (A) 1D and (B) 2D ^{1}H-NMR spectra for **5** (300 MHz, CD_3CN).

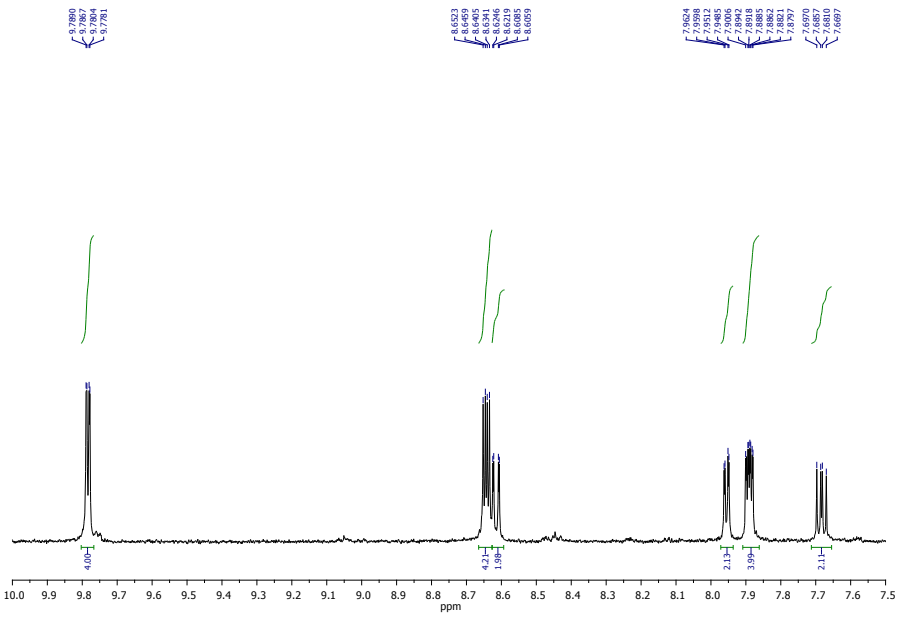

Figure S12. 1D ^{1}H-NMR spectrum for **6** (500 MHz, CD_3CN).

6. HRMS spectra and data

Measured Mass

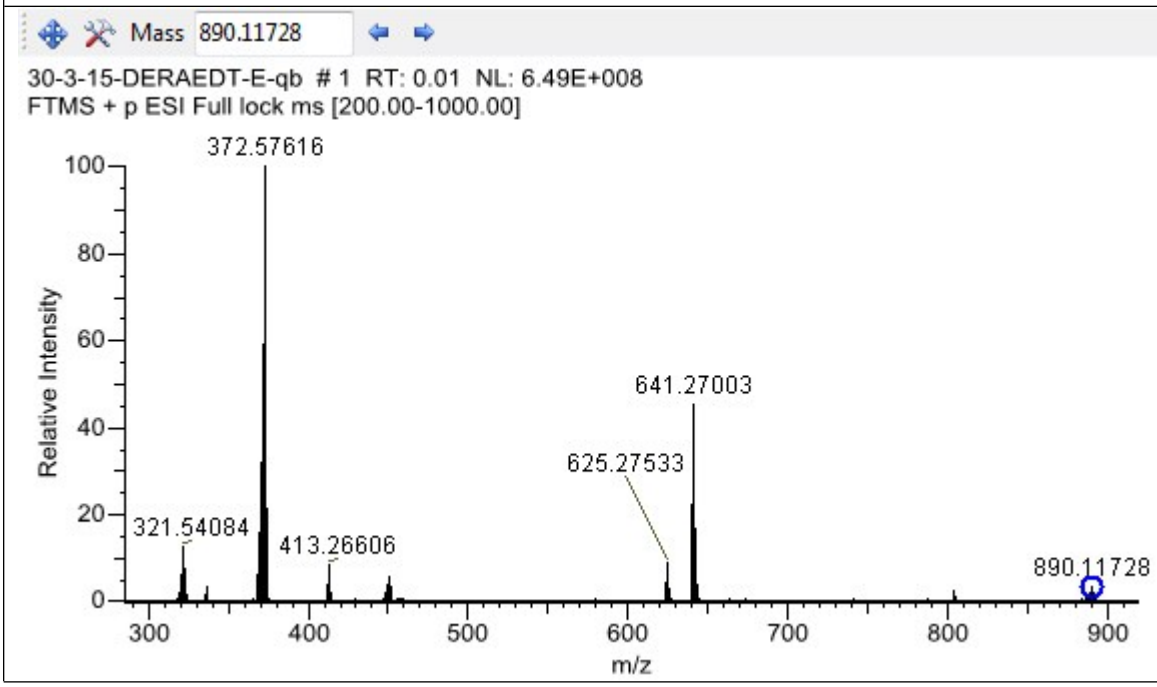

Calculated Mass

Spectral Fit: 100.00
Max dM: 5.00[Ppm] max dI 20.00% Threshold 0.16

Mass	Intensity[%]	dM[Ppm]	dI[%]	Fit[%]	Contrib[%]
884.11967	14.2	-0.22	0.14	100.00	100.00
885.12285	6.9	-0.03	-0.34	100.00	100.00
886.11834	5.4	-0.23	-0.73	100.00	100.00
887.11817	34.9	-0.04	-0.18	100.00	100.00
888.11773	44.7	-0.14	-0.34	100.00	100.00
889.11832	61.0	-0.24	1.63	100.00	100.00
890.11731	100.0	-0.04	0.00	100.00	100.00
891.12003	43.3	-0.20	-0.90	100.00	100.00
892.11813	54.5	-0.23	-0.16	100.00	100.00
893.12089	24.1	-0.29	0.31	100.00	100.00
894.12395	5.6	-0.22	-0.49	100.00	100.00
895.12707	0.8	1.45	-0.77	100.00	100.00

Formula

Mass	Intensity	Intensity[%]	Resolution
890.11728	22254576	3	68045

Mass	Composition	Fit
890.11643	$C_{43}H_{29}N_7F_6P_1{}^{102}Ru_1$	100.00

Figure S13. HRMS data for **1** ([M-PF_6^-]$^+$).

Measured Mass

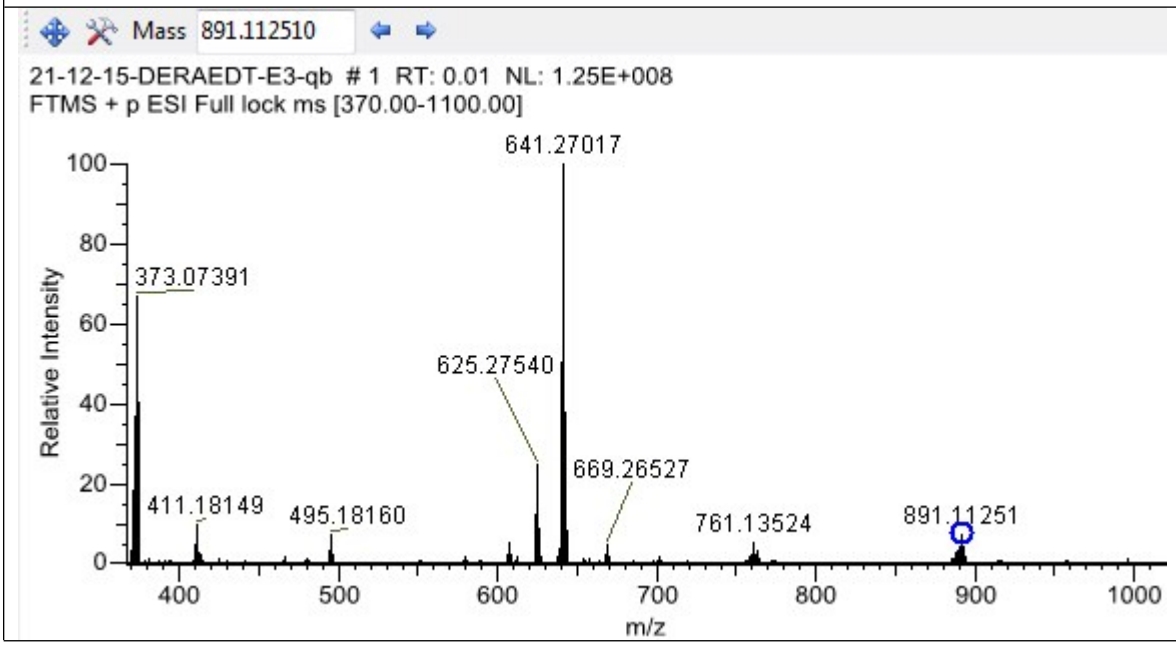

Calculated Mass

Spectral Fit: 100.00
Max dM: 5.00[Ppm] max dI 20.00% Threshold 0.09

Mass	Intensity[%]	dM[Ppm]	dI[%]	Fit[%]	Contrib[%]
885.11492	14.3	-0.08	-0.01	100.00	100.00
886.11808	6.7	-0.07	-0.40	100.00	100.00
887.11355	5.4	0.01	-0.78	100.00	100.00
888.11343	35.0	-0.10	0.73	100.00	100.00
889.11294	44.7	-0.17	-1.82	100.00	100.00
890.11355	60.8	-0.08	-0.96	100.00	100.00
891.11255	100.0	-0.04	0.00	100.00	100.00
892.11523	42.5	-0.22	-0.11	100.00	100.00
893.11335	54.5	-0.02	-0.71	100.00	100.00
894.11609	23.6	-0.03	-0.13	100.00	100.00
895.11913	5.4	-0.06	-0.34	100.00	100.00
896.12220	0.8	1.18	-0.47	100.00	100.00

Formula

Mass	Intensity	Intensity[%]	Resolution
891.112510	9291717	7	67521

Mass	Composition	Fit
891.111675	$C_{42}H_{28}N_8F_6P_1{}^{102}Ru_1$	100.00

Figure S14. HRMS data for **2** ($[M\text{-}PF_6^-]^+$).

Measured Mass

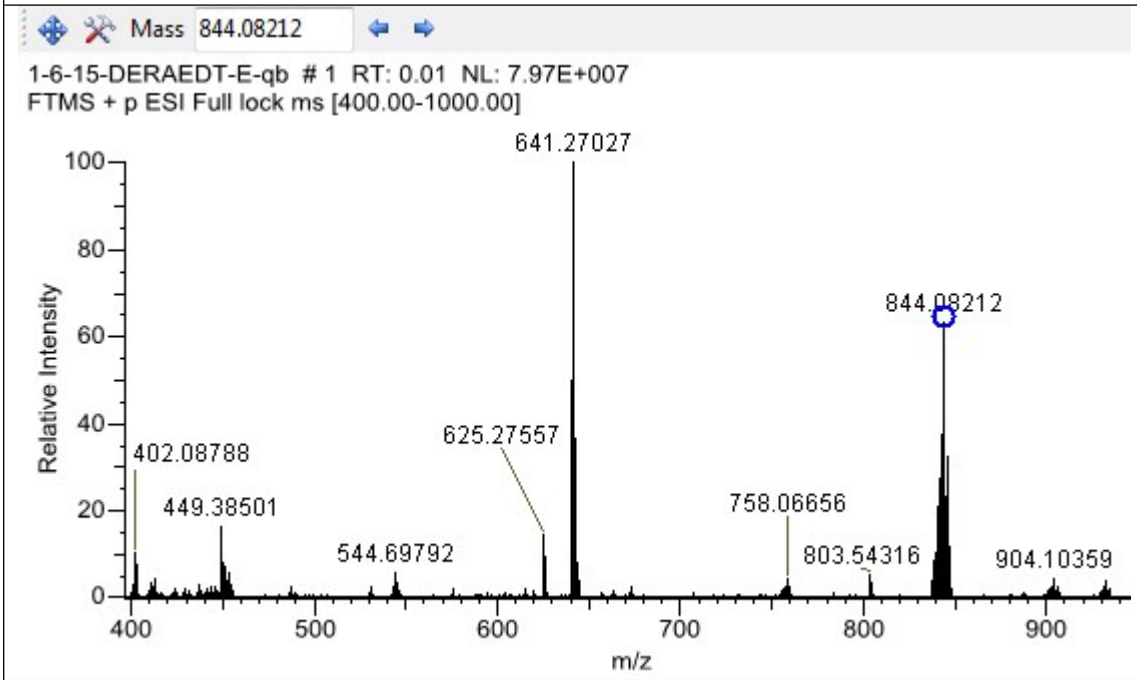

Calculated Mass

Spectral Fit: 100.00
Max dM: 5.00[Ppm] max dI 20.00% Threshold 0.01

Mass	Intensity[%]	dM[Ppm]	dI[%]	Fit[%]	Contrib[%]
838.08502	14.8	0.31	-1.45	100.00	100.00
839.08807	5.9	0.16	-0.84	100.00	100.00
840.08324	5.4	0.33	-0.82	100.00	100.00
841.08348	36.0	0.00	-2.95	100.00	100.00
842.08274	43.9	0.21	-1.38	100.00	100.00
843.08347	60.2	-0.20	-1.80	100.00	100.00
844.08242	100.0	-0.35	0.00	100.00	100.00
845.08512	36.7	-0.80	-0.38	100.00	100.00
846.08321	54.6	-0.37	-3.24	100.00	100.00
847.08601	20.6	-0.68	-2.18	100.00	100.00
848.08895	4.0	-0.72	-0.51	100.00	100.00
849.09188	0.5	-0.90	-0.08	100.00	100.00
850.09476	0.0	-1.15	-0.04	100.00	100.00

Formula

Mass	Intensity	Intensity[%]	Resolution
844.08212	50908448	64	71056

Mass	Composition	Fit
844.08177	$C_{35}H_{23}N_{11}F_6P_1{}^{102}Ru_1$	100.00

Figure S15. HRMS data for **3** ($[M-(PF_6)^-]^+$).

Measured Mass

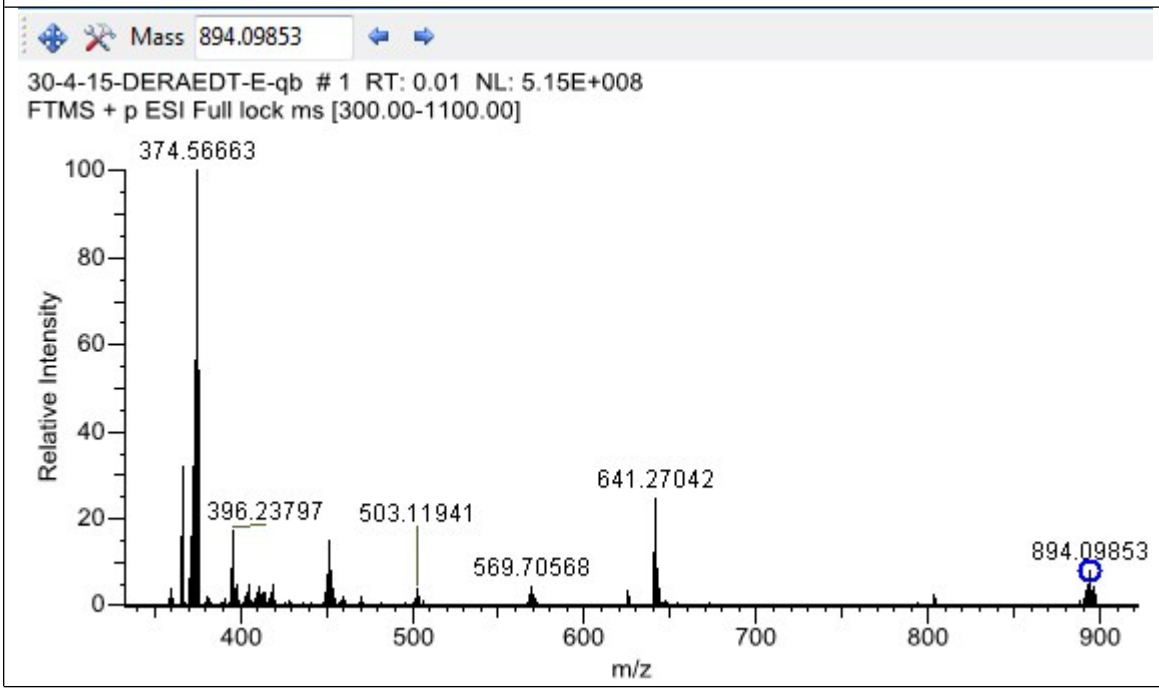

Calculated Mass

Spectral Fit: 100.00
Max dM: 5.00[Ppm] max dI 20.00% Threshold 0.08

Mass	Intensity[%]	dM[Ppm]	dI[%]	Fit[%]	Contrib[%]
888.10067	14.4	0.29	-0.75	100.00	100.00
889.10373	6.4	0.14	-0.80	100.00	100.00
890.09913	5.5	0.55	-0.53	100.00	100.00
891.09915	35.3	0.18	-1.30	100.00	100.00
892.09856	44.4	0.42	-1.87	100.00	100.00
893.09921	60.5	0.14	0.55	100.00	100.00
894.09820	100.0	0.38	0.00	100.00	100.00
895.10084	40.3	0.17	0.23	100.00	100.00
896.09899	54.5	0.24	-2.46	100.00	100.00
897.10171	22.5	0.18	-0.99	100.00	100.00
898.10464	4.8	0.31	-0.70	100.00	100.00
899.10759	0.7	0.49	-0.41	100.00	100.00

Formula

Mass	Intensity	Intensity[%]	Resolution
894.09853	41395020	8	69758

Mass	Composition	Fit
894.09742	$C_{39}H_{25}N_{11}F_6P_1{}^{102}Ru_1$	100.00

Figure S16. HRMS data for **4** ($[M-(PF_6)^-]^+$).

Measured Mass

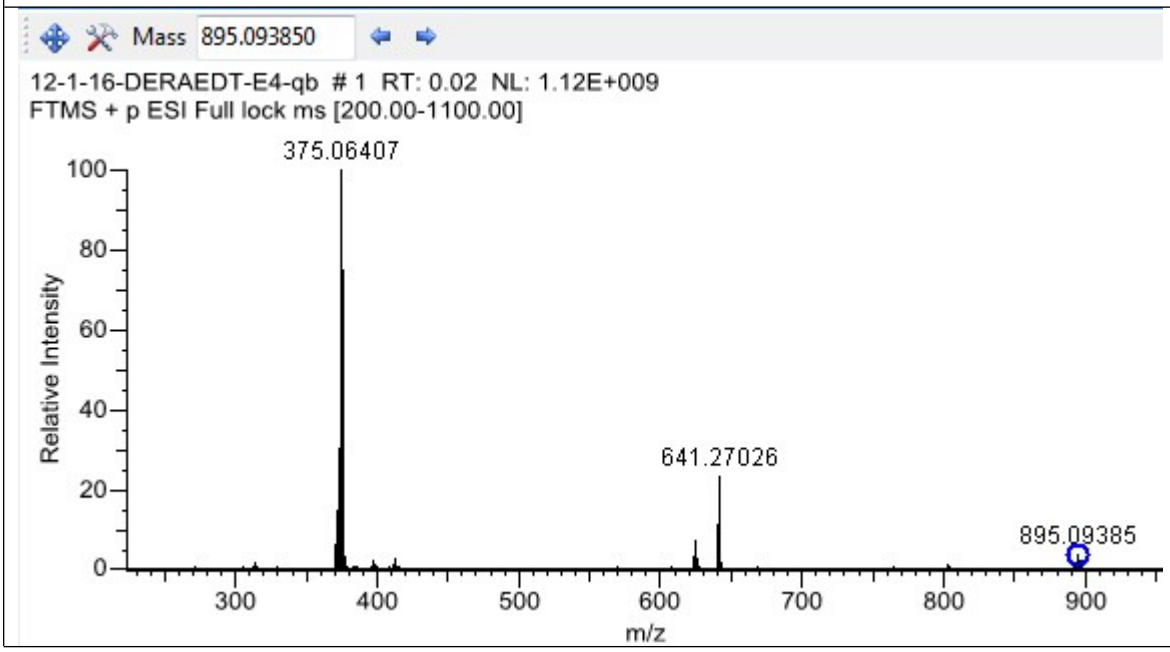

Calculated Mass

Spectral Fit: 100.00
Max dM: 5.00[Ppm] max dI 20.00% Threshold 0.10

Mass	Intensity[%]	dM[Ppm]	dI[%]	Fit[%]	Contrib[%]
889.09592	14.4	0.30	-2.87	100.00	100.00
890.09892	6.3	-0.15	-2.59	100.00	100.00
891.09445	5.5	-0.30	-1.61	100.00	100.00
892.09439	35.2	0.34	-1.84	100.00	100.00
893.09380	44.5	0.44	-2.61	100.00	100.00
894.09445	60.3	0.45	0.90	100.00	100.00
895.09344	100.0	0.45	0.00	100.00	100.00
896.09603	39.6	0.13	2.81	100.00	100.00
897.09424	54.5	0.45	-2.98	100.00	100.00
898.09690	22.1	0.20	-2.56	100.00	100.00
899.09977	4.6	0.14	-0.72	100.00	100.00
900.10264	0.6	1.67	-0.53	100.00	100.00

Formula

Mass	Intensity	Intensity[%]	Resolution
895.093850	44825764	4	66244

Mass	Composition	Fit
895.092671	$C_{38}H_{24}N_{12}F_6P_1{}^{102}Ru_1$	100.00

Figure S17. HRMS data for **5** ($[M-(PF_6)^-]^+$).

7. Cyclic voltammograms for the Ru(II) complexes

Recorded in dry acetonitrile under argon, with a sweep rate of 0.3 V/s, at room temperature. The concentration of the complexes is 8.10^{-4} mol/L, with 0.1 mol/L tetrabutylammonium perchlorate as supporting electrolyte.

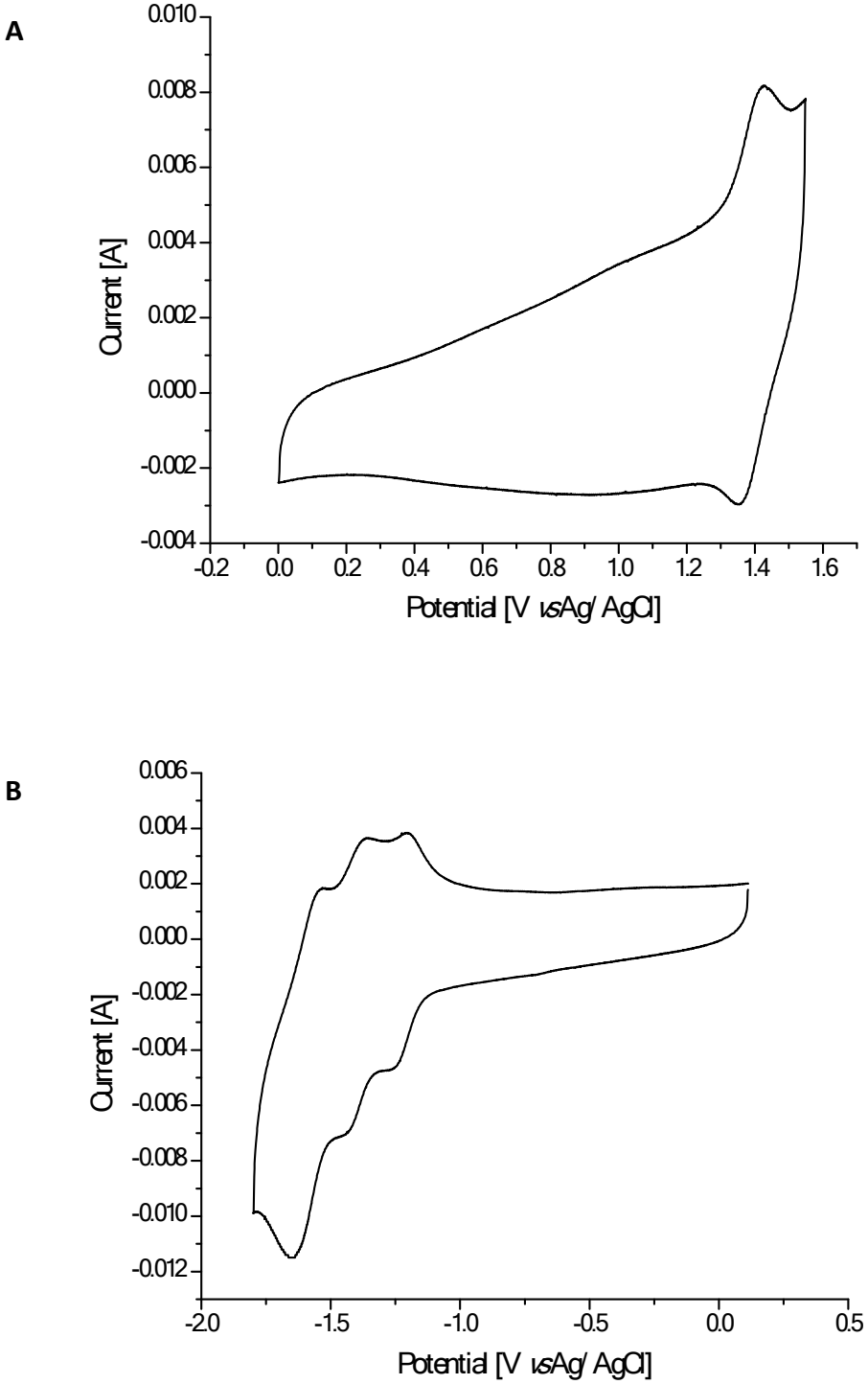

Figure S18. Cyclic voltammograms of **1**. (A) Positive polarization; (B) negative polarization.

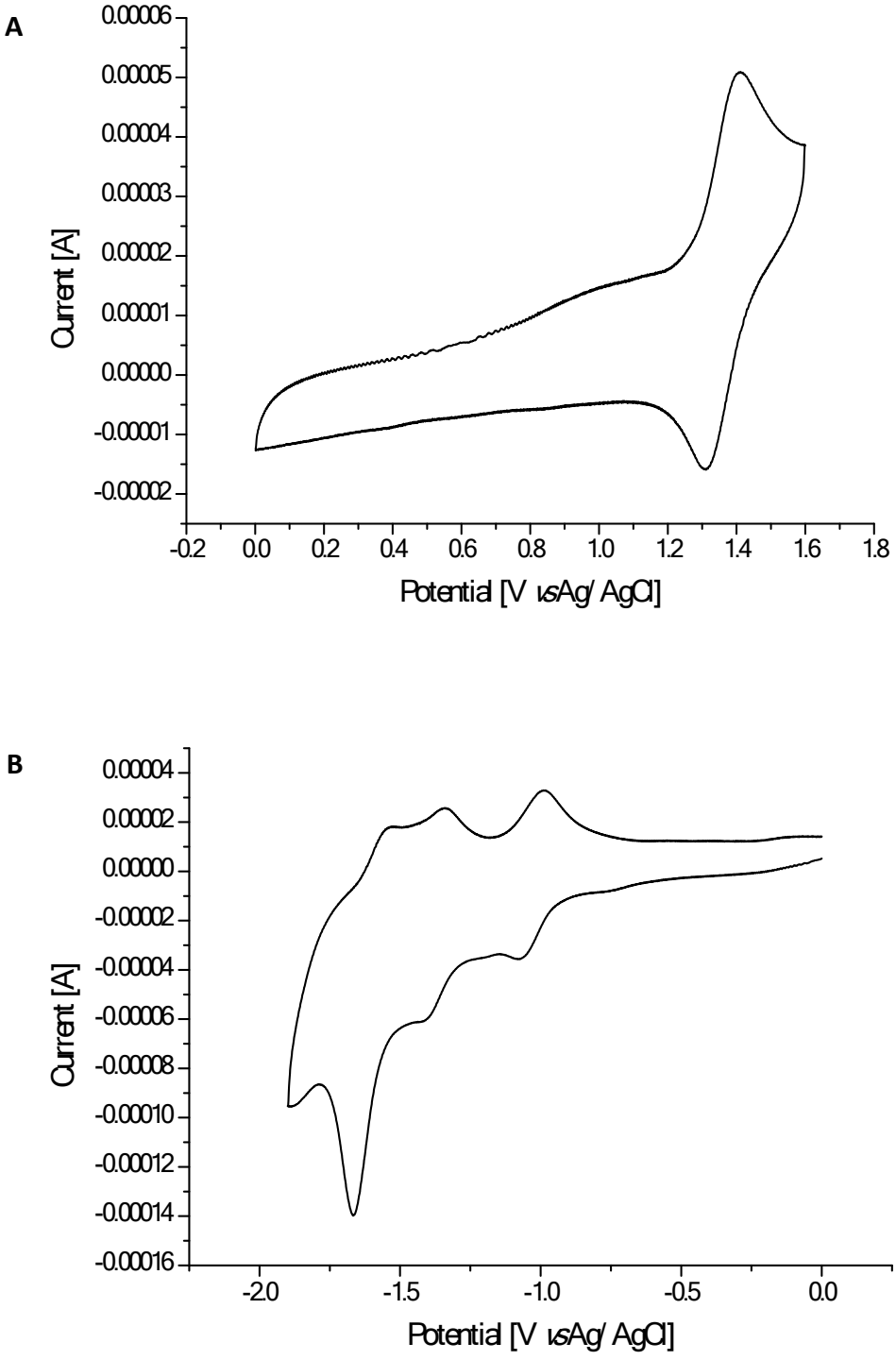

Figure S19. Cyclic voltammograms of **2**. (A) Positive polarization; (B) negative polarization.

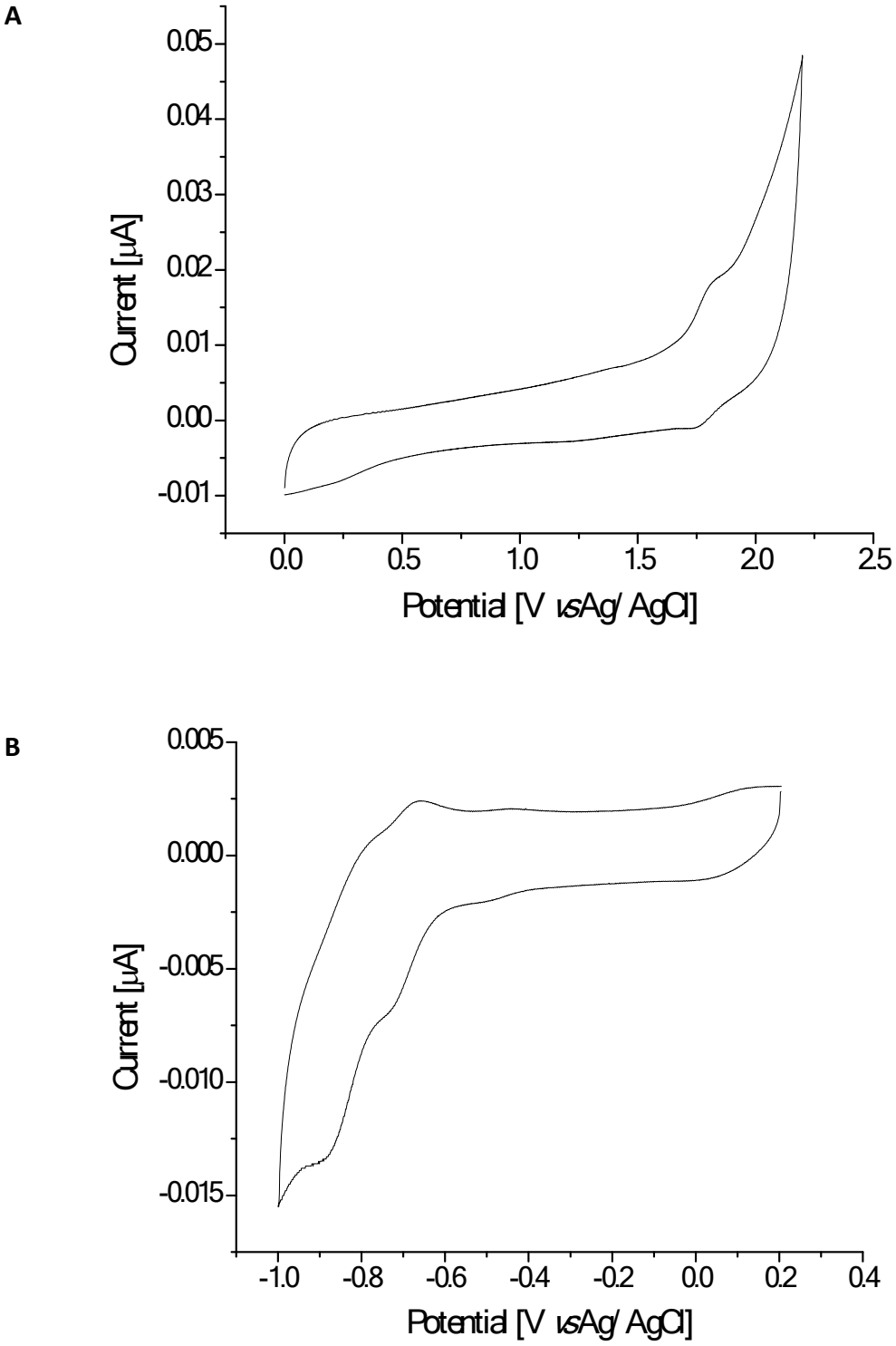

Figure S20. Cyclic voltammograms of **3**. (A) Positive polarization; (B) negative polarization.

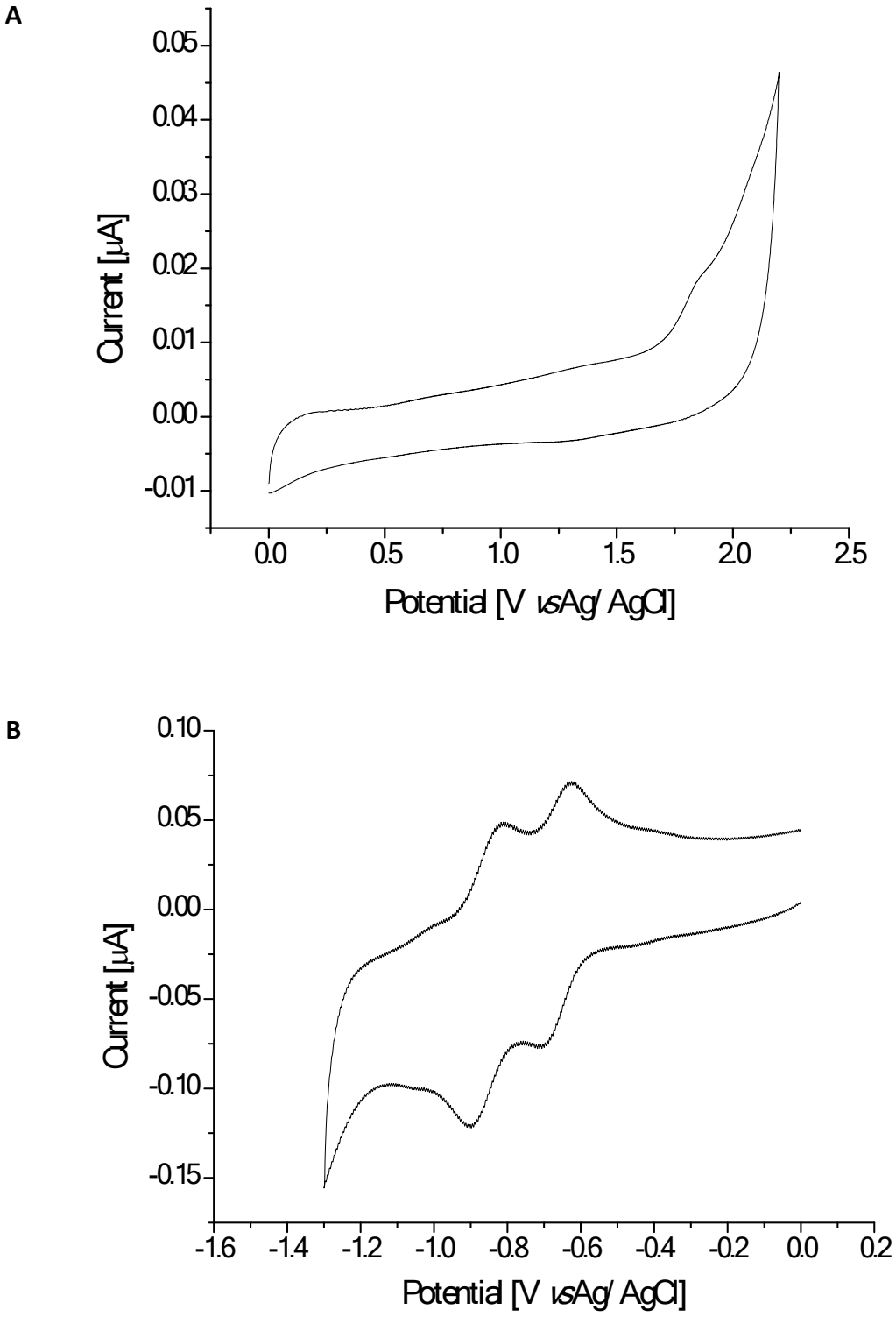

Figure S21. Cyclic voltammograms of **4**. (A) Positive polarization; (B) negative polarization.

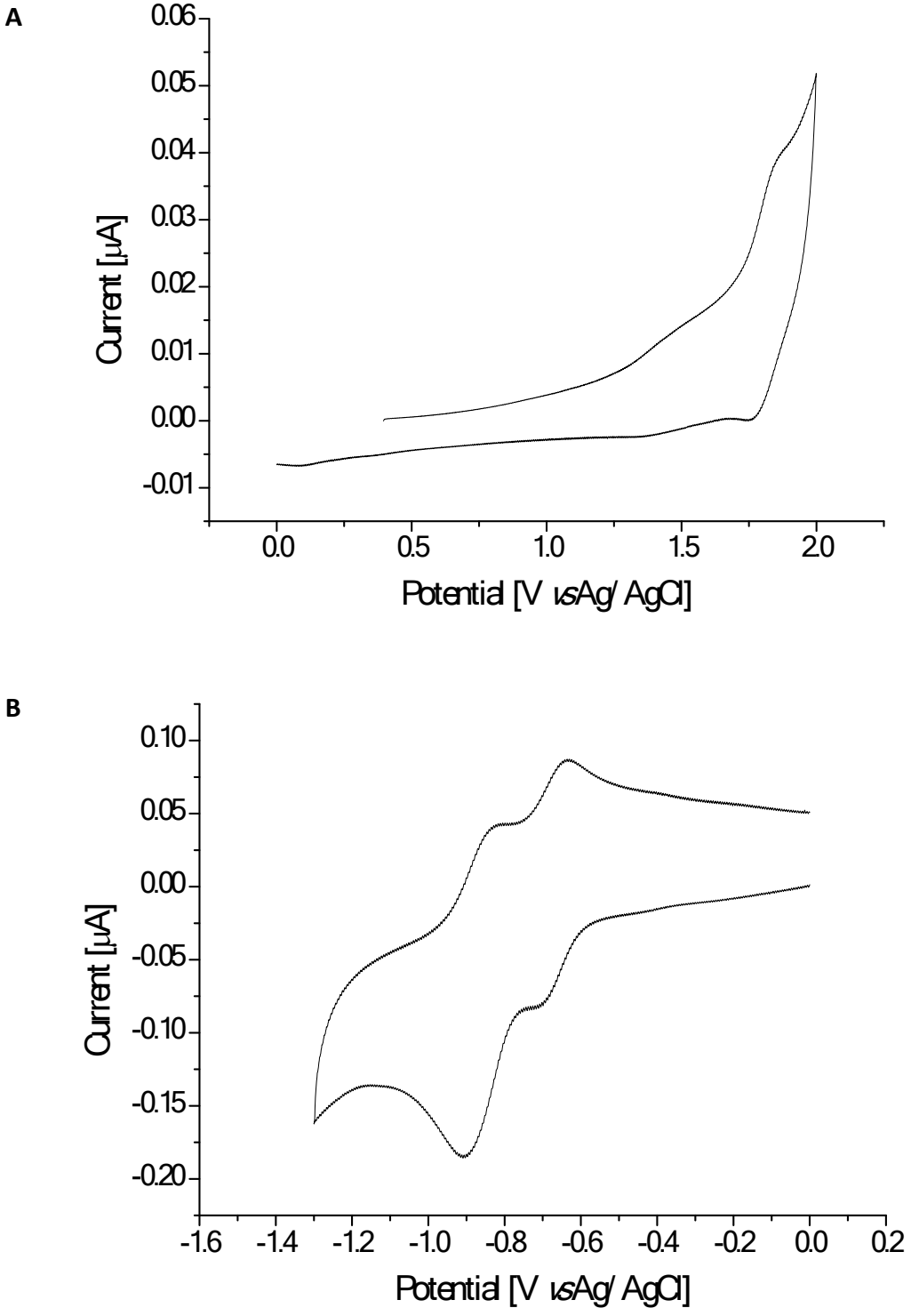

Figure S22. Cyclic voltammograms of **5**. (A) Positive polarization; (B) negative polarization.

8. Emission spectra of complexes 1 and 2 in the presence of dGMP

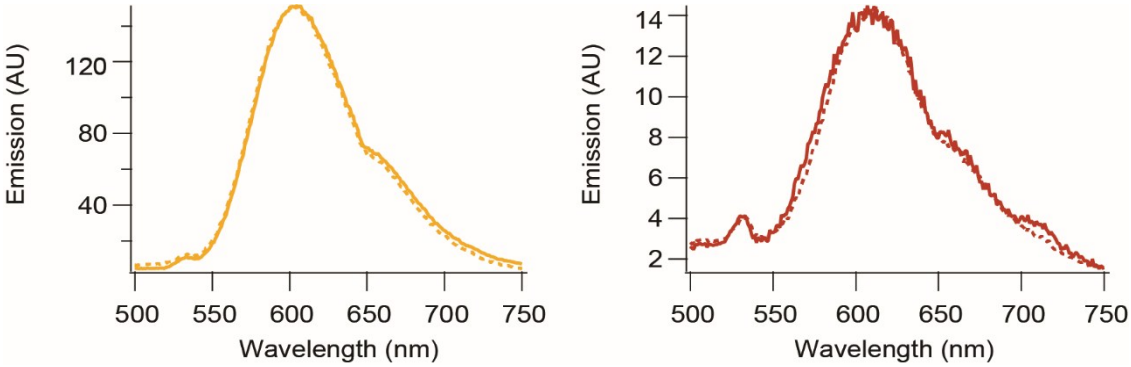

Figure S23. Steady-state luminescence spectra of **1** (left) and **2** (right) in the absence (full line) or the presence of 10 mM dGMP (dashed line). Measurements made in TRIS.HCl 5 mM, NaCl 50 mM, pH = 7.4, under ambient air conditions.

9. Hairpin Mismatch-containing titration experiments

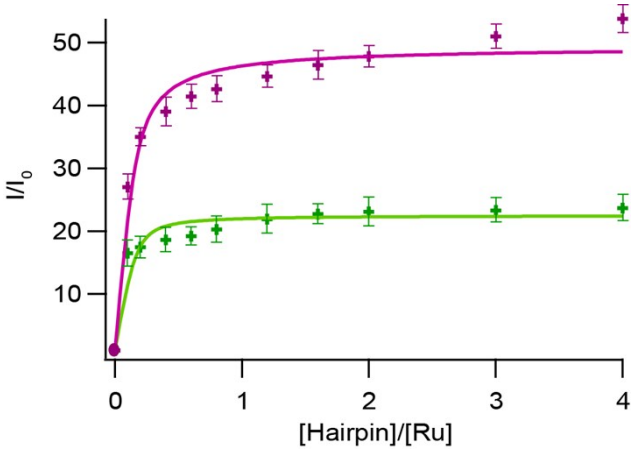

Figure S24. Steady-state luminescence titration of **2** with hairpin oligonucleotides fully matched (green) or containing a CC mismatched base pair (purple). Measurements are performed using 1 µM of complex in Tris.HCl buffer 5 mM, NaCl 1 mM, pH 7.5 under ambient air conditions. The fitted curved are obtained by global fitting on the whole data set.

Titrations of **2** with the well-matched and mismatched duplexes (Figure S23) were used to estimate the binding affinity of the complex for well-matched and mismatched sites. In order to evaluate this binding affinity, we must consider two competing equilibria, expressed below, for the intercalation of the complex at well-matched sites (eq.1) and insertion at the mismatch site (eq.2).

$$C + BP \rightleftharpoons [C\_BP] \qquad K_{ass} = \frac{[C\_BP]}{[C]\,[BP]} \qquad \text{(eq.1)}$$

$$C + MM \rightleftharpoons [C\_MM] \qquad K_{MM} = \frac{[C\_MM]}{[C]\,[MM]} \qquad \text{(eq.2)}$$

where K_{ass} describes the binding equilibrium between the complex, *C*, and the well-matched base pair sites, *BP*, in the DNA, and K_{MM} describes the binding equilibrium between the complex and the mismatched site, *MM*.

The total concentration of complex as C_C; this is kept constant throughout the titration. We can then define the various molar fractions for the complex as follows:

$f = \frac{[C]}{C_C}$, the molar fraction of free complex.

$b = \frac{[C\_BP]}{C_C}$, the molar fraction of complex bound to WM base pairs.

$m = \frac{[C\_MM]}{C_C}$, the molar fraction of complex bound to MM sites.

Additionally, we express the total concentration of hairpin as C_{ODN}; this value increased throughout the titration. The variable *R* is introduced as being equal to the ratio C_{ODN}/C_C, and in our titration the luminescence of the complex is measured as a function of this ratio *R*. The ratio of luminescence intensity, I/I_0, can be expressed as a function of *R* as follows:

$$I/I_0 = f + \alpha\, b + \beta\, m \quad \text{(eq.3)}$$

where α and β are equal to the relative emissivity of complex associated with *BP* and *MM*, respectively.

Two other parameters are defined: *x*, the ratio of mismatched sites per base pairs in the duplex, and *p*, the occupational factor which takes into account the possible inhibition of intercalation of two complexes in close vicinity. *n* represents the total number of base pairs in the hairpin. We are now ready to express the equilibrium concentrations of free BP and MM sites as follows:

$$[BP] = n\,(1-x)\,C_{ODN} - p\,[C_{BP}] = n\,(1-x)\,C_{ODN} - p\,b\,C_C \quad \text{(eq.4)}$$

$$[MM] = n\,x\,C_{ODN} - [C\_MM] = n\,x\,C_{ODN} - m\,C_C \quad \text{(eq.5)}$$

Thus,

$$\frac{[BP]}{C_C} = n\,(1-x)\,R - p\,b \quad \text{and} \quad \frac{[MM]}{C_C} = n\,x\,R - m$$

The binding equilibrium equations are thus rewritten as:

$$K_{ass} = \frac{b}{f\,C_C(n\,(1-x)\,R - p\,b)} \quad \text{and} \quad K_{MM} = \frac{m}{f\,C_C(n\,x\,R - m)}$$

The expression of *b* and *m* as functions of *f* can thus be obtained:

$$K_{ass}\,f\,C_C(n\,(1-x)\,R - p\,b) - b = 0 \quad \text{(eq.6)}$$

$$b = \frac{K_{ass}\,f\,C_C\,n\,(1-x)\,R}{1 + p\,K_{ass}\,f\,C_C} \quad \text{(eq.7)}$$

$$K_{MM}\,f\,C_C(n\,x\,R - m) - m = 0 \quad \text{(eq.8)}$$

$$m = \frac{K_{MM}\,f\,C_C\,n\,x\,R}{1 + K_{MM}\,f\,C_C} \quad \text{(eq.9)}$$

With

$$1 = f + b + m \quad \text{(eq.10)}$$

$$0 = f - 1 + \frac{K_{ass}\,f\,C_C\,n\,(1-x)\,R}{1 + p\,K_{ass}\,f\,C_C} + \frac{K_{MM}\,f\,C_C\,n\,x\,R}{1 + K_{MM}\,f\,C_C} \quad \text{(eq.11)}$$

$$0 = (f-1)\left(1 + p\,K_{ass}\,f\,C_C\right)\left(1 + K_{MM}\,f\,C_C\right) + K_{ass}\,f\,C_C\,n\,(1-x)\,R\,(1 + K_{MM}\,f\,C_C) + K_{MM}\,C_C\,n\,x$$

(eq.12)

The expression of the ratio of the intensity of luminescence, I/I_0, can be expressed as follows:

$$I/I_0 = f + \alpha\frac{K_{ass}\,f\,C_C\,n\,(1-x)\,R}{1 + p\,K_{ass}\,f\,C_C} + \beta\frac{K_{MM}\,f\,C_C\,n\,x\,R}{1 + K_{MM}\,f\,C_C} \quad \text{(eq.13)}$$

The fitting process using eq.13 is realized by an iterative solving to the expression of *f* using the eq.12. Moreover, a global fitting approach is used to fit the data on both the CC mismatch sequencence and the well-matched sequence. The binding affinity K_{ass} and the factors p and α are linked for the global

fit. In the case of the well-matched sequence (*x*=0), the parameters K_{MM} and β are kept constant at 1 and 0 respectively.

The parameters obtained after global fit (occupational factor set to 2) depicted in Figure S23 are presented in the following table. The binding affinity for the mismatch sites obtained using the global fitting process is evaluated to be one order magnitude larger than the binding affinity for well-matched base pairs.

	Global Fit [a]	**AT Hairpin**	**CC Hairpin**
K_{ass} (L/mol)	Linked	3.88 10^6	
K_{MM} (L/mol)	Free	(1)	1.42 10^7
x	Fixed	(0)	(0.0833)
p [b]	Linked	(2)	
α	Linked	22.50	
β	Free	(0)	130.0

[a] Parameters in parenthesis are kept fixed during the global fitting process. [b]The best fit is obtained with the occupational factor *p* equal to 2.

We want to draw the attention of the lector on the fact that these binding affinities are indicative on the binding processes between complex **2** and mismatched and well-matched site. Indeed, a deviation from the theoretical plateau can be observed at high [Hairpin]/[Ru] ratio. These deviations can be rationalized by the fact that: (i) we used a racemic mixture of complex **2**; the Δ or the Λ enantiomer of the complex could be assumed to interact differently with DNA sites, for both the affinity and the luminescence enhancement, which will introduce deviation from the theoretical model. (ii) For comparison purpose, we used hairpin DNA broadly reported in literature for screening the sensitivity of probes for mismatched sites. Nevertheless, the T-loop could also be a binding site for the complex, which is not taken into account in the model. In conclusion, we would like to stress that the binding values reported in the previous table are indicative and are used to give an insight on the binding process.

Similar titration experiments were realized using the photoreactive complex **5** (Figure S24). Due to the presence of G base close to the mismatched or well-matched site, an interpretation of this titration is more complex. However, the slightly more efficient quenching observed in the case of the AA and CC mismatches compared to the well-matched sequence supports the preference of insertion of **5** in these former sites.

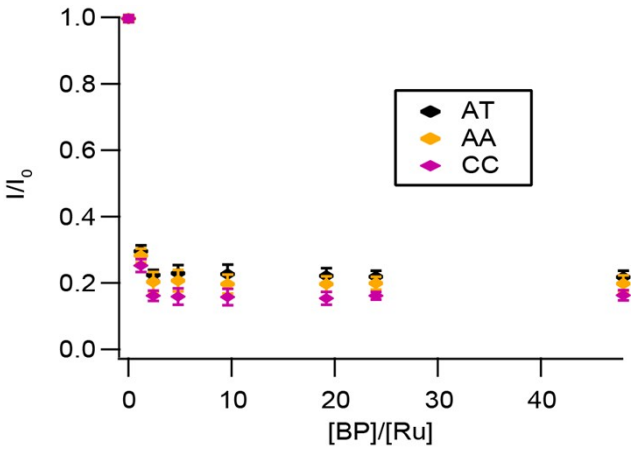

Figure S25. Steady-state luminescence titration of **5** with hairpin oligonucleotides fully matched (black) or containing either a AA (yellow) or a CC (purple) mismatched base pair. Measurements are performed using 1 µM of complex in Tris.HCl buffer 5 mM, NaCl 1 mM, pH 7.5 under ambient air conditions.